JOURNAL OF VIROLOGY, Mar. 2009, p. 2584–2591 Vol. 83, No. 6
0022-538X/09/$08.00+0 doi:10.1128/JVI.02158-08

Role of Conserved Cysteines in the Alphavirus E3 Protein▽

Megan M. Parrott,[1] Sarah A. Sitarski,[1]† Randy J. Arnold,[2] Lora K. Picton,[3] R. Blake Hill,[3] and Suchetana Mukhopadhyay[1]*

Department of Biology[1] and Department of Chemistry,[2] Indiana University, 212 S. Hawthorne Drive, Bloomington, Indiana 47405, and Department of Biology, The Johns Hopkins University, 3400 N. Charles St., Baltimore, Maryland 21218[3]

Received 13 October 2008/Accepted 18 December 2008

Alphavirus particles are covered by 80 glycoprotein spikes that are essential for viral entry. Spikes consist of the E2 receptor binding protein and the E1 fusion protein. Spike assembly occurs in the endoplasmic reticulum, where E1 associates with pE2, a precursor containing E3 and E2 proteins. E3 is a small, cysteine-rich, extracellular glycoprotein that mediates proper folding of pE2 and its subsequent association with E1. In addition, cleavage of E3 from the assembled spike is required to make the virus particles efficiently fusion competent. We have found that the E3 protein in Sindbis virus contains one disulfide bond between residues Cys19 and Cys25. Replacing either of these two critical cysteines resulted in mutants with attenuated titers. Replacing both cysteines with either alanine or serine resulted in double mutants that were lethal. Insertion of additional cysteines based on E3 proteins from other alphaviruses resulted in either sequential or nested disulfide bond patterns. E3 sequences that formed sequential disulfides yielded virus with near-wild-type titers, while those that contained nested disulfide bonds had attenuated activity. Our data indicate that the role of the cysteine residues in E3 is not primarily structural. We hypothesize that E3 has an enzymatic or functional role in virus assembly, and these possibilities are further discussed.

Alphaviruses are members of the *Togaviradae* family and are single-stranded, positive-sense RNA, enveloped viruses (17). The lipid membranes of the viruses have 80 glycoprotein spikes which are required for viral entry. Each spike is comprised of three copies of a heterodimer which consists of the E2 and E1 proteins (22, 54). E2 and E1 are glycoproteins with a single transmembrane helix that traverses the host-derived lipid bilayer. E2 interacts with the nucleocapsid core at the C terminus (12, 16, 27, 43) and contains the receptor binding site at the N terminus (5, 21, 45). E1 is the viral fusion protein responsible for mediating fusion between the virus membrane and the host cell membrane during an infection (13, 39, 47). Specific interactions in both the ectodomain and transmembrane regions are critical for heterodimer formation (30, 35, 46, 54). The assembly of each heterodimer, its subsequent assembly into a spike, and the interaction of the cytoplasmic tail of the spike with the nucleocapsid core are all essential for the efficient production of infectious particles.

Glycoprotein spike assembly requires four structural proteins, E3, E2, 6K, and E1, which are expressed as a single polyprotein. E3 is a small, 64-amino-acid protein (Sindbis virus [SINV] numbering) and contains a signal sequence that translocates the protein into the endoplasmic reticulum (ER) (3, 4, 15). Early in translation, glycosylation of N14 (SINV numbering) occurs and this promotes E3's release from the ER membrane into the lumen. As a result, the signal sequence is not cleaved from the E3 protein (14). Cellular enzymes cleave the polyprotein to yield pE2 (an uncleaved protein consisting of E3 and E2), 6K, and E1 (23, 55) proteins. In the ER, E1 is found in several conformations, only one of which will form a functional heterodimer with pE2, allowing its transport to the Golgi apparatus (1, 2, 6, 7, 36). After pE2-E1 heterodimerization, self-association between three heterodimers occurs and each individual spike is formed (25, 26, 36). As observed with Semliki Forest virus, disulfide bonds reshuffle within pE2 during protein folding (34), possibly forming intermolecular disulfide bonds between E3 and E2 residues. However, no intermolecular disulfide bonds between pE2 and E1 have been identified (34). Once the viral spikes have been assembled, they are transported to the plasma membrane (11) and are thus exposed to subcellular changes of pH, from pH 7.2 in the ER to pH 5.7 in the vesicles constitutively transporting the spikes to the plasma membrane. In the trans-Golgi network, the E3 protein is cleaved from pE2 by the cellular protein furin (18, 44, 55). E3 remains noncovalently attached to the released virus particle, while in other species E3 is found in the medium of virus-infected cells (32, 49).

E3 is required for efficient particle assembly, both in mediating spike folding and in spike activation for viral entry. When an ER signal sequence was substituted for the E3 protein, heterodimerization of pE2 and E1 was abolished (26). Furthermore, when E2 and E1 were expressed individually, low levels of E2 were transported to the cell surface while E1 remained in the ER, suggesting that heterodimerization with pE2 is necessary for E1 to be transported to the cell surface (24, 26, 46). These results are consistent with E3 playing a critical role in mediating the folding of pE2 and the association of pE2 and E1 proteins during spike assembly (7, 38). In viruses where the furin cleavage site was mutated, the virus particles were correctly assembled but severely reduced in infectivity, presumably because the fusion protein was unable to dissociate from pE2 and initiate fusion (44, 55).

* Corresponding author. Mailing address: Department of Biology, Indiana University, 212 S. Hawthorne Drive, Bloomington, IN 47405. Phone: (812) 856-3686. Fax: (812) 856-5710. E-mail: sumukhop@indiana.edu.

† Present address: Wells Center for Pediatric Research, 1044 W. Walnut St., R4-431B, Indianapolis, IN 46202.

▽ Published ahead of print on 24 December 2008.

```
                  *  ◊    *       *                              *
SINV  SAAPLVT-AMCLLGNVSFPCDRP---PTCYTREPSRALDILEENVNHEAYDTLLNAILRCGSSGRSKR 64
SFV   -SAPLIT-AMCVLANATFPCFQPPCVPCCYENNAEATLRMLEDNVDRPGYYDLLQAALTCRNGTRHRR 66
RRV   -SAALM---MCILANTSFPCSSPPCYPCCYEKQPEQTLRMLEDNVNRPGYYELLEASMTCRNRSRHRR 64
BFV   SAAALXITALCVLQNLSFPCDAPPCAPCCYEKDPAGTLRLLSDHYYHPKYYELLDSTMHCPQGRRPKR 68
EEE   ---SLAT-VMCVLANITFPCDQPPCMPCCYEKNPHETLTMLEQNYDSRAYDQLLDAAVKCNAR-RTRR 63
ONN   -SLALP--VMCLLANTTFPCSQPPCAPCCYEKKPEETLRMLEDNVMQPGYYQLLDSALACSQR-RQKR 64
IGB   -SLALP--VMCLLANTTFPCSQPPCAPCCYEKKPEETLRMLEDNVMQPGYYQLLDSALACSQH-RQRR 64
OCK   SAAPLVT-AMCLLGNVSFPCNRP---PTCYTREPSRALDILEENVNHEAYDTLLNAILRCGSSGRSKR 64
WEE   ----LVT-ALCVLSNVTFPCDKP---PVCYSLAPERTLDVLEENVDNPNYDTLLENVLKCPSR-RPKR 59
AUR   --SRAIT-AMCILQNVTFPCDRP---PTCYNRNPDLTLTMLETNVNHPSYDVLLDAALRCPTR-RHVR 61
VEE   ---SLVT-TMCLLANVTFPCAEP---PICYDRKPAETLAMLSVNVDNPGYDELLEAAVKCPGR-KRR- 59
```

FIG. 1. E3 amino acid sequence alignment from a representative group of alphaviruses. The cysteines marked with asterisks are conserved in all alphavirus species. The ◊ indicates the conserved but nonessential glycosylation site. The PPCXPCC motif present in ~50% of alphaviruses is underlined. SFV, Semliki Forest virus; RRV, Ross River virus; BFV, Barmah Forest virus; EEE, eastern equine encephalitis virus; ONN, O'nyong nyong virus; IGB, Igbo Ora virus; OCK, Ockelbo virus; WEE, western equine encephalitis virus; AUR, Aura virus; VEE, Venezuelan equine encephalitis virus.

A comparison of an amino acid sequence alignment of E3 proteins from different alphaviruses (Fig. 1) shows that the E3 protein is a small protein with four conserved cysteine (Cys) residues. A subset of E3 proteins contains an additional two Cys residues in a narrow cysteine/proline-rich region, PPCXPCC (Fig. 1). We have purified recombinant E3 protein from SINV and have determined that a disulfide bond is present and, furthermore, that these Cys residues are important in virus assembly. Within the alphavirus E3 proteins, we have identified a region that is important for mediating spike transport to the plasma membrane and thus is critical for spike assembly.

MATERIALS AND METHODS

Viruses and cells. All virus mutations were made in a full-length cDNA TE12 clone of SINV (28). BHK-21 cells (American Type Tissue Culture, Manassas, VA) were grown in minimal essential medium (Gibco Life Technologies, Carlsbad, CA) supplemented with 10% fetal bovine serum (Atlanta Biologicals, Lawrenceville, GA) at 37°C in the presence of 5% CO_2.

E3 cloning, expression, and purification. E3 from SINV was cloned into a SUMO expression vector (courtesy of Thomas Bernhardt, Harvard Medical School, Boston, MA) and transformed into Rosetta gami 2 (Novagen, Darmstadt Germany) chemically competent cells. For large-scale expression of the SUMO-E3 fusion protein, referred to as SUMO-E3, cells were grown in Terrific Broth medium supplemented with ampicillin at a final concentration of 100 μg/ml and chloramphenicol at a final concentration of 37 μg/ml at 37°C. When the optical density at 600 nm reached 0.4 to 0.6, cells were induced with IPTG (isopropyl-β-D-thiogalactopyranoside) at a final concentration of 1 mM, shifted to 16°C, and grown for an additional 18 h. Cells were pelleted at 4,500 × *g* for 15 min at 4°C. Cell pellets were resuspended in 5 ml buffer A (20 mM phosphate [pH 8], 300 mM NaCl, 10 mM imidazole) per 1 g cell pellet. A protease inhibitor cocktail tablet (Roche Diagnostics, Indianapolis, IN) was added. Cells were lysed with two passages through a French pressure cell at 12,000 lb/in^2 (SLM-Aminco, Urbana, IL) or three passages through a continuous-flow microfluidizer (Micro-Fluidics, Taylorsville, UT). Unlysed cells and insoluble material were pelleted at 125,000 × *g* for 30 min. The clarified lysate was filtered using a 0.2-μm syringe filter and loaded onto a HisTrap FF Crude column (1 ml) (GE Healthcare, Piscataway, NJ). Protein was eluted by a step gradient made from buffer A and buffer B (20 mM phosphate [pH 8], 300 mM NaCl, 300 mM imidazole). Fractions corresponding to SUMO-E3 were concentrated and buffer exchanged into 20 mM phosphate (pH 8) and 300 mM NaCl using 3K Amicon Ultra concentrators (Millipore, Billerica, MA) at 5,000 × *g* at 4°C. The SUMO-E3 protein was digested with SUMO protease (courtesy of Thomas Bernhardt, Harvard Medical School, Boston, MA) for 48 h at 4°C and loaded onto HisTrap HP (1 ml). Fractions containing E3 elute in the flowthrough, while SUMO and the SUMO protease remain bound to the column. Isolated E3 proteins were concentrated as described above. Isolated E3 protein concentration and purity were determined by the standard Bradford assay and 10 to 20% Tris-Tricine sodium dodecyl sulfate-polyacrylamide gel electrophoresis (SDS-PAGE).

CD. Circular dichroism (CD) measurements were carried out in a J-715 CD spectropolarimeter (JASCO), which is equipped with a PTC-343 Peltier-type cell holder for temperature control. E3 samples were prepared in 20 mM phosphate buffer (pH 8) and 100 mM NaF. CD spectra from 190 nm to 260 nm were recorded in a 1-mm-path-length cuvette at 10°C.

Gel filtration. Purified E3 protein was loaded onto a Superdex peptide HR 10/30 column (GE Amersham, Piscataway, NJ) equilibrated in 20 mM phosphate (pH 8) and 300 mM NaCl. The sample was eluted from the column at 0.5 ml/min, and fractions were analyzed using 10 to 20% Tris-Tricine SDS-PAGE.

Expression of ^{15}N-labeled E3 and nuclear magnetic resonance (NMR) spectroscopy. To produce uniformly ^{15}N-labeled E3, SUMO-E3 was grown in M9 minimal medium containing $^{15}NH_4Cl$ (1 g/liter; Cambridge Stable Isotopes, Andover, MA) as described previously (29). The remainder of the purification of ^{15}N SUMO-E3 and E3 was the same as described above.

Two-dimensional ^{1}H-^{15}N heteronuclear single-quantum coherence (HSQC) spectra were collected at 600 MHz on a Bruker Avance II spectrometer outfitted with a cryoprobe at 298 K using Watergate for solvent suppression (41). A uniformly ^{15}N-labeled E3 sample was prepared by extensive buffer exchange into 20 mM phosphate and 100 mM NaCl with a pH of 7.4 with no correction following the addition of 10% D_2O. The protein concentration in the sample used for NMR experiments was 0.1 mM, and 32 scans were collected for each t1 increment with a total of 64 t1 increments.

Liquid chromatography-tandem mass spectrometry (LC-MS/MS) and data interpretation. Five nanograms of purified E3 was treated under reducing conditions (12.5 mM dithiothreitol [DTT] [Sigma Aldrich, St. Louis, MO] and 125 mM ammonium bicarbonate [Mallinckrodt Baker Inc, Paris, KY]) and nonreducing conditions (phosphate-buffered saline [PBS]) for 2 h at 37°C. Free cysteines were alkylated in 10 mM iodoadetamide for 90 min at 27°C. Samples were incubated in chymotrypsin (Sigma Aldrich, St. Louis, MO) for 18 h at 37°C. The reactions were quenched with 1% formic acid (Sigma Aldrich, St. Louis, MO).

Six microliters of digested protein was loaded onto a C_{18} reversed-phase trapping column (15-mm, 100-μm-inner-diameter capillary packed with 5 μm Magic C18AQ particles with 200-Å pore size; Michrom Bioresources, Auburn, CA) and washed with about 20 μl solvent A (3% acetonitrile, 0.1% formic acid). Peptides were separated by elution through a 15-cm reversed-phase nanoLC column (75-μm-inner-diameter capillary pulled to a tip and packed with 5 μm Magic C18AQ particles with 100-Å pore size; Michrom Bioresources) by increasing solvent B (0.1% formic acid in acetonitrile) from 5% to 40% at 250 ml/min over 30 min and electrosprayed directly into the source of an ion trap mass spectrometer which recorded mass spectra and data-dependent tandem mass spectra of the peptide ions (LCQ Deca XP; ThermoFinnigan, San Jose, CA). Data-dependent tandem mass spectra were recorded by acquiring a precursor mass spectrum followed by two tandem mass spectra of the two most intense ions from the precursor scan (unless excluded by the dynamic exclusion algorithm, in which case the next most abundant ions were selected). Spectra either were automatically interpreted using the database searching tool Mascot v. 1.9 (Matrix Science, Boston, MA) and manually validated or were manually interpreted (as for peptides containing disulfide bonds).

Generation of mutant virus stocks. Cysteine and PPCXPCC motif mutations in TE12 cDNA clones were introduced using QuikChange site-directed mutagenesis (Stratagene, La Jolla, CA), and the genes corresponding to the E3 and E2 proteins were sequenced. Mutant cDNA clones were linearized with SacI and

in vitro transcribed with SP6 RNA polymerase (40). For electroporation, ~10^8 BHK cells were trypsinized, washed twice in PBS, and resuspended in a final volume of 500 μl PBS. Cells were combined with in vitro-transcribed RNA in a 2-mm-gap cuvette and were pulsed once at 1.5 kV, 25 μF, and 200 Ω using the Bio-Rad Gene Pulser Xcell electroporation system. After a 10-min recovery at room temperature, cells were diluted 1:10 in minimal essential medium with 10% fetal bovine serum. Virus was harvested ~24 h postelectroporation, and the titer was determined using standard plaque assay procedure (40).

Immunofluorescence staining for E2 expression. BHK-21 cells were transfected with viral RNA using Lipofectamine 2000 (Invitrogen, Carlsbad, CA) according to the manufacturer's protocol. To view E2 expression at the plasma membrane, cells were fixed with 1.5% paraformaldehyde (Electron Microscopy Science, Hatfield, PA) at 6 h posttransfection for 20 min at room temperature. Following fixation, cells were washed with 1× PBS and stained with a polyclonal antibody against E2 (Cocalico, Reamstown, PA) and the secondary antibody Alexa Flour 488 (Invitrogen, Carlsbad, CA). Nuclei were stained with 10 μg/ml DAPI (4′,6′-diamidino-2-phenylindole) (Sigma Aldrich, St Louis, MO). To view E2 expression in the cytoplasm, BHK cells were fixed and permeabilized in 1.5% paraformaldehyde and 0.01% Triton X-100 at 10 h posttransfection for 20 min at room temperature and stained for E2 and DAPI. All washes and incubations were performed with 1× PBS plus 0.01% Triton X-100 at room temperature.

Revertant screening. Mutant viruses were serially passaged over BHK cells, and plaque size was monitored to indicate a potential second-site revertant. Genomic RNA was isolated from large plaques that had been passaged once (40). Reverse transcription-PCR was performed on the region of the genome corresponding to the structural proteins, and mutations were identified. In order to verify that the larger-plaque phenotype was due to the specific mutation, the revertant site was introduced into the mutant virus, and plaque sizes and growth kinetics of the mutant virus, the isolated revertant, the mutant virus containing the revertant site, and wild-type virus were determined.

RESULTS

Expression, purification, and characterization of recombinant E3 protein. To characterize the properties of E3, we recombinantly expressed the protein in bacteria. The glycosylation site on SINV E3 was shown to be dispensable for virus production (C. Melki and S. Mukhopadhyay, data not shown), consistent with results for other deglycosylation mutants (42). E3 was expressed and purified as a His-tagged SUMO fusion. Incubation of the SUMO-E3 protein with a SUMO-specific protease cleaved the E3 protein from the SUMO-E3 protein (Fig. 2A, inset) at the first residue of the E3 protein. Gel filtration of the recombinant E3 protein on a Superdex peptide column showed that the protein elutes primarily as a single peak at an elution volume corresponding to a ~7-kDa protein (Fig. 2A) that was confirmed as E3 by MS analysis.

E3 is predicted to have a high alpha-helical content (Fig. 2B). This was confirmed experimentally using far-UV CD (Fig. 2C). To evaluate the tertiary structure of SINV E3, a ^{15}N HSQC spectrum was obtained. The spectrum showed monodisperse peaks with good chemical shift dispersion, suggesting a monomeric, folded protein (Fig. 2D). Approximately 10% of the chemical shifts are consistent with random-coil values, indicating that part of the E3 protein is unstructured. NMR line shape analysis indicated similar line widths for the majority of cross peaks, indicating that the E3 protein was predominantly in a single oligomeric state (Fig. 2D), consistent with gel filtration results (Fig. 2A).

Identification of disulfide bonds in recombinant E3. There are four conserved Cys residues in alphaviruses (Fig. 1). In SINV, these residues are Cys10, Cys19, Cys25, and Cys56. To assess whether these cysteines were involved in disulfide bond formation, we used chemical modification followed by LC-MS/MS. We treated E3 under native (no DTT) and reduced (12.5 mM DTT) conditions, coupling free thiols with iodoacetamide, digesting the protein with chymotrypsin, and then examining the peptides by LC-MS/MS. Analysis of the data (an example is shown in Fig. 3) confirms the presence of a disulfide bond between Cys19 and Cys25 in the SINV E3 protein. Under native conditions, we observed that the peptide GNSFPC-DRPPTCY (covering residues 14 to 26) was not alkylated, indicating that Cys19 and Cys25 were buried or formed an intrapeptide disulfide. Based on the mass of the peptide, the latter possibility is favored. Peptides containing Cys10 and Cys56 show that these residues were alkylated, suggesting that they do not form disulfide bonds in E3. In contrast, when E3 was incubated under reducing conditions, Cys19 and Cys25 were alkylated. Data of similar quality (not shown) have also been obtained for the peptide covering residues 12 to 26 and also verify the presence of a disulfide bond between Cys19 and Cys25.

A small percentage of the sample shows that Cys10 and Cys56 form a disulfide bond, but this is not the predominant species and, as shown below, is not biologically relevant.

Mutational analysis of cysteine residues in SINV. Possible roles for the Cys19 and Cys25 residues are (i) to form a structurally essential disulfide bond, (ii) to have an enzymatic/functional role during virus assembly, or (iii) both. To investigate the role of Cys19 and Cys25 in virus assembly, Cys mutations were made in SINV and infectivity was determined (Table 1). Cys was substituted with both Ser and Ala to ensure that the phenotype observed was not due to the nature of the amino acid or its size. Both amino acid substitutions showed similar trends (Table 1). Single-site mutations of Cys19 and Cys25 resulted in virus with lower titers and smaller plaque sizes than wild-type virus, indicating that the presence of at least one of these two cysteines is important in virus assembly but that both are not essential. The double Cys19 Cys25 mutant was not viable, and no infectious virus was recovered. Immunofluorescence assays indicated that E2 protein was being translated but not transported to the cell membrane in the double mutants (data not shown).

As a control, the C56S mutant, which does not form a disulfide bond in recombinant SINV E3, had infectivity levels comparable to those of wild-type virus. The Cys10 mutants had a lower titer than the wild type, but these mutations change the ER signal sequence, reducing the total amount of spike proteins and virus particles being synthesized.

It is interesting that a single-site Cys mutation still yielded infectious particles, suggesting that the virus utilizes alternative mechanisms for disulfide bond formation during assembly. This alternative pathway(s), however, is not sufficient when both Cys19 and Cys25 are mutated.

Characterization of recombinant E3 protein containing the PPCXPCC motif. Our results indicate that Cys residues in E3 have a functional rather than a structural role. In a subset of alphaviruses, the E3 protein contains a Pro-Cys-rich region, the PPCXPCC motif. We examined the effect of each Cys residue in the PPCXPCC motif on disulfide bond formation by generating SINV E3 mutants that contained the entire PPCXPCC motif or part of the motif (Fig. 4 and Table 2). SINV E3+PCV+C contained the entire PPCVPCC motif and introduced two additional Cys residues. SINV E3+PCV and SINV E3+C each contained part of the motif with one additional Cys

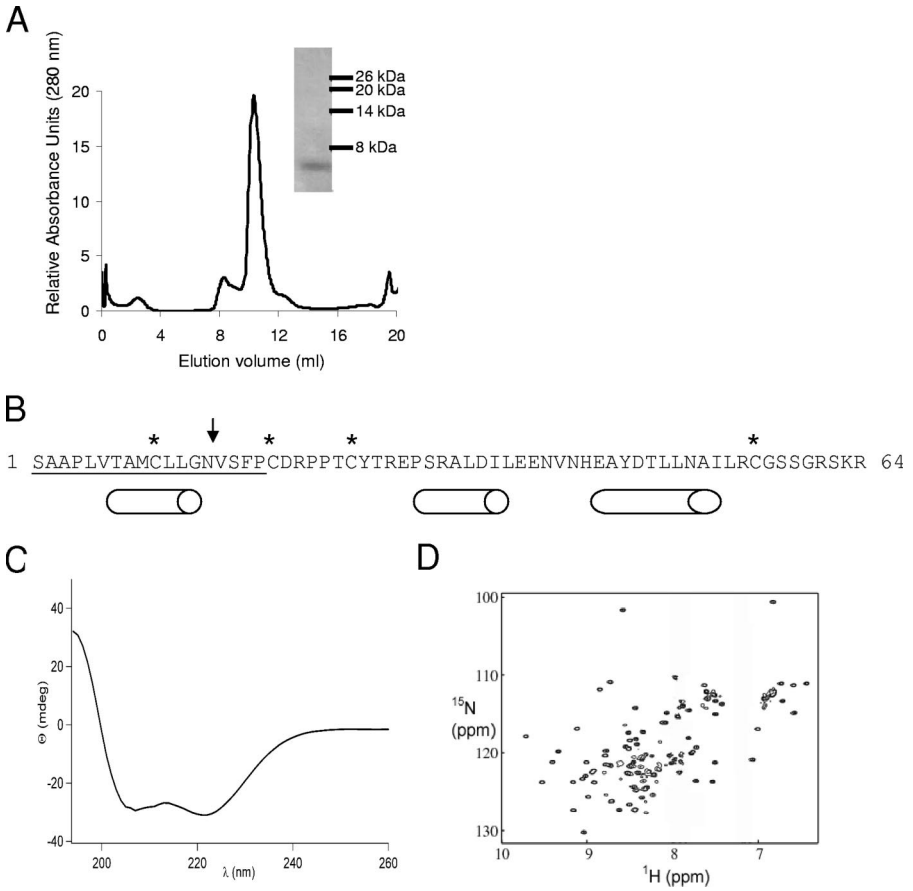

FIG. 2. Expression and characterization of SINV E3 protein. (A) Gel filtration profile of SINV E3. E3 was eluted from a Superdex peptide HR 10/30 column at a flow rate of 0.5 ml/min. Comparison with a calibration curve shows that a majority of the protein elutes at ~7 kDa, the size of an E3 monomer. Inset, SDS-PAGE showing concentrated SINV E3 after Superdex peptide column elution. Molecular mass of E3, 7 kDa. (B) Amino acid sequence of SINV E3 protein. The N-terminal signal sequence that is responsible for *trans*-localization of E3-E2-6K-E1 to the lumen of the ER is underlined, the conserved glycosylation site is indicated by the arrow, and the four cysteine residues conserved in all alphaviruses are marked with asterisks. Cylinders represent regions of predicted alpha helices as determined by JPred (10). (C) Representative CD spectrum of purified SINV E3 protein. Purified E3 was prepared in 20 mM phosphate buffer (pH 8) and 100 mM NaF, and an average of three spectra from 190 nm to 260 nm were recorded in a 1-mm-path-length cuvette. The minima at 208 and 220 nm indicate alpha-helical secondary structures, consistent with secondary structure prediction (Fig. 2C). (D) ^{1}H-^{15}N-HSQC of SINV E3. A proton-nitrogen NMR correlation spectrum of 100 μM E3 at 600 MHz, 25°C, and pH 7.5 (20 mM PO_4 buffer, 100 mM NaCl) is shown. The well-dispersed chemical shifts indicate that E3 is well folded. The line widths are typical for a monomeric globular protein of the size of E3, which is consistent with gel filtration results (panel A).

residue. To keep the amino acid numbering consistent, SINV E3 numbering is used. To indicate the inserted "PCV" residues in SINV+PCV and SINV+PCV+C, these are referred to as insP, insC, and insV and follow residue Pro22 in SINV E3. An amino acid substitution of T24C was made to generate the "+C" component in SINV+C and SINV+PCV+C mutants, and this is referred to as Cys24.

The recombinant proteins were expressed to similar levels as SINV E3 and were purified in a similar manner. The disulfide bonds in these E3 proteins were determined as for recombinant SINV E3. The pattern of disulfide bonds in SINV E3 and the PPCXPCC mutants can be divided into two groups: sequential and nested disulfide bonds (Fig. 4). SINV+PCV+C and SINV+C both had two sets of sequential disulfide bonds; Cys19-insC and Cys24-Cys25 in SINV+PCV+C, and Cys10-Cys19 and Cys24-Cys25 in SINV+C (Fig. 4). In contrast, SINV+PCV contained nested disulfide bonds, Cys10-Cys25 and Cys19-insC (Fig. 4).

The insertion of a single Cys residue (T24C), present in SINV+PCV+C and SINV+C, did not disrupt protein function but rather induced the formation of a disulfide bond between two adjacent Cys residues (Cys24-Cys25). While vicinal disulfides are rare, these bonds are not unprecedented (8, 9, 19, 20, 48) and are energetically acceptable (53). Other proteins with vicinal disulfide bonds are involved in redox processes or are regulated by redox events, suggesting that this bond is transient as pE2 travels through the secretory system.

Role of the PPCXPCC motif in virus. In order to determine if the disulfide bond pattern seen in E3 correlated with infectivity of mutant virus, the SINV+PCV+C, SINV+PCV, and SINV+C mutations were made in SINV (Table 2). SINV+PCV+C and SINV+C had titers comparable to those of wild-

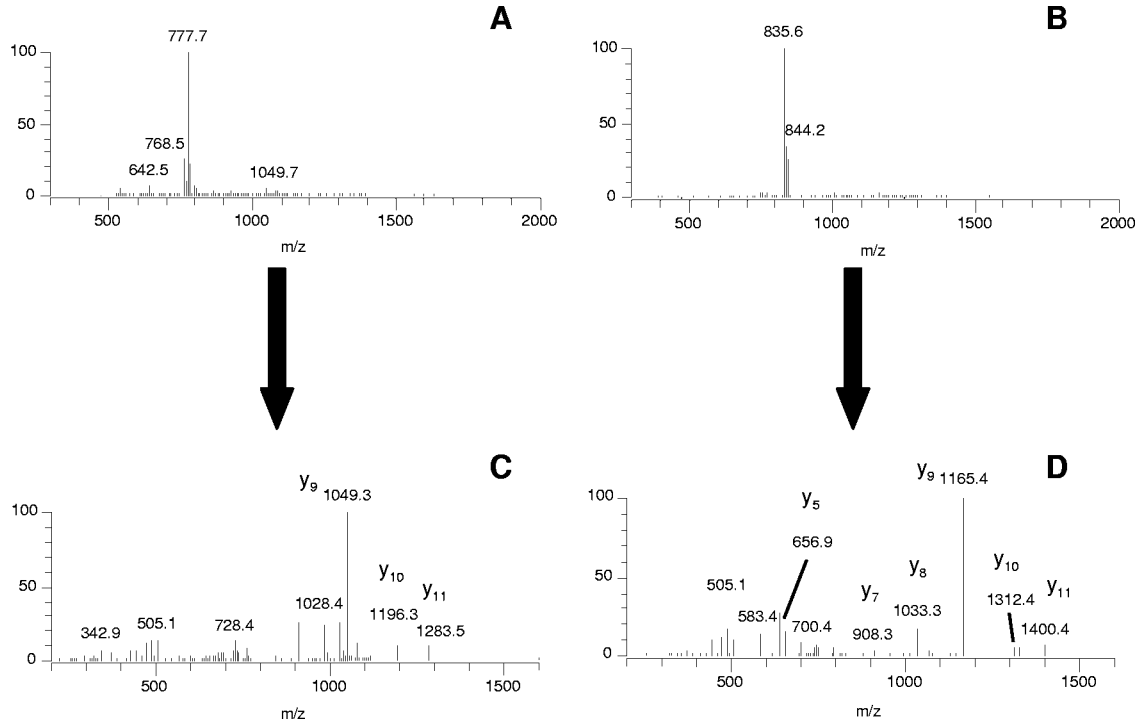

FIG. 3. An example of disulfide bond identification as determined by chemical modification and LC-MS/MS analysis. MS analysis of the peptide GNSFPCDRPPTCY (covering residues 14 to 26) of SINV E3 under nonreduced conditions is shown in panels A and C, and that under reduced conditions is shown in panels B and D. Under nonreduced conditions, the *m/z* for the doubly charged GNSFPCDRPPTCY precursor peptide is 777.7. The same peptide under reduced conditions has a double-charge *m/z* of 835.6. Initial base peak chromatograms showed good separation for both the nonreduced and reduced samples. Furthermore, selected ion chromatograms showed a distinct peak corresponding to each precursor peptide (data not shown). Data-dependent tandem mass spectra were recorded by acquiring a precursor mass spectrum followed by two tandem mass spectra of the two most intense ions from the precursor scan. (A) Mass spectrum showing the intact precursor under nonreduced conditions with *m/z* 777.7. (B) Mass spectrum showing the intact precursor under reduced conditions with *m/z* 835.6. In both spectra the precursor is the main component, indicating that no other peptide fragments were coeluted. (C) The tandem mass spectrum of the *m/z* 777.7 precursor (nonreduced samples). (D) The tandem mass spectrum of the *m/z* 835.6 precursor (reduced samples). The sequence-specific fragment ions in both panels C and D are labeled y_5 to y_{11}, and all match the calculated *m/z* values, consistent with the disulfide bond being retained in these fragments (C) or with the absence of a disulfide bond and the two Cys residues being alkylated (D).

type SINV indicating that Cys24 by itself does not play a critical role in virus assembly. However, insertion of PCV alone resulted in very little to no infectious virus particles being released. Comparing the in vivo infectivity results with the disulfide bond pattern in the E3 protein, all the mutants that are viable in vivo have disulfide bond patterns that contain one or more sequential disulfide bonds. The SINV+PCV mutant is not viable, and the E3 protein containing this mutation consists of two disulfide bonds that are nested one within another (Fig. 4). Immunofluorescence assays showed that pE2 was expressed but that very small amounts were transported to the plasma membrane (Fig. 5). These results were confirmed by pulse-chase experiments which showed that the amount of E2 at the cell surface of PCV-transfected cells is severely reduced compared to that in wild-type virus (data not shown). Improper folding of pE2, a result of misfolded E3, would severely affect the heterodimerization between pE2 and E1.

TABLE 1. Infectivities of SINV E3 cysteine mutants[a]

SINV	Titer (PFU/ml)	Plaque size (mm) after 24 h
Wild type	4.5×10^9	4
C56S	6.2×10^9	4
C19S	1.9×10^5	2
C19A	2.8×10^8	1
C25S	7.2×10^4	2
C25A	4.5×10^7	1
C19S C25S	No infectious particles	
C19A C25A	No infectious particles	

[a] BHK-21 cells were electroporated with equal amounts of in vitro-transcribed RNA. Virus was harvested at 24 h after electroporation, and titers were determined by plaque assay.

Isolation and identification of a second-site revertant for SINV+PCV. The yield of SINV+PCV infectious particles was attenuated, and the plaque phenotype was small. Serial passaging of this mutant virus over BHK cells led to isolation of a large plaque that was comparable in size to wild-type SINV. The RNA sequence from the isolated large plaque revealed a second-site reversion at position E3 T24P (Table 2), creating PPCVPPC, in contrast to PPCVPTC found in SINV+PCV. This revertant grew at titers comparable to those of wild-type SINV, and the cellular localization of pE2/E2 was similar to that of wild-type SINV, SINV+PCV+C, and SINV+C virus (data not shown). When the T24P second-site revertant site

FIG. 4. Disulfide bonds present in E3 PPCXPCC motif mutants determined by chemical modification and LC-MS/MS analysis. Disulfide bonds between Cys residues in the E3 protein of the PPCXPCC motif mutants are indicated with a curved bracket. A horizontal line is drawn over the PPCXPCC motif, the four conserved cysteines in E3 are in red, and portions of the PPCXPCC motif that were introduced into SINV E3 are shown in green. The second-site reversion site, T24P, isolated from the SINV+PCV mutant is shown in blue in the sequence marked SINV+PCV+P. Each E3 protein was processed and analyzed as described in the legend to Fig. 3 and in the text.

was introduced into SINV+PCV virus (named SINV+PCV+P [Table 2]), this mutant grew to a wild-type titer, confirming that this single residue could enhance viral infectivity.

The disulfide bond pattern of the SINV+PCV+P E3 protein was determined, and two sequential disulfide bonds were identified. Cys10 and Cys19 formed one bond, while residues insC and Cys25 formed another (Fig. 4). As seen with other infectious mutants, sequential disulfide bonds were present.

The reversion of T24P now creates a PPCXPPC sequence, in contrast to PPCXPCC, in the virus, suggesting that the Pro-Pro residues may be a structural substitute for the vicinal disulfide bonds seen in SINV+C and SINV+PCV+C. The corresponding T→P mutation was made in SINV, and surprisingly, this mutant, SINV+P, grew like wild-type virus (Table 2) even though the E3 protein now contained three consecutive Pro residues.

DISCUSSION

E3 is a key player in alphavirus spike assembly but is not required for viral entry. Although E3 had previously been isolated from the medium of virus-infected cells (32, 49), the protein was denatured during the purification, and as a result, no structural information about E3 was obtained. In this study, by using a combination of mutant viruses and recombinant E3 protein, fundamental structural information about E3 was obtained. Analysis of these results allows us to hypothesize about a possible function of the E3 protein, as discussed below.

E3 is a small, extracellular protein that contains multiple conserved Cys residues. Two Cys residues, Cys19 and Cys25, in recombinant SINV E3 are involved in disulfide bond formation. E3 lacking either Cys19 or Cys25 had reduced infectivity, and if both residues were deleted, the virus was noninfectious. It is interesting to note that the C→S and C→A single-site mutants both had attenuated titers compared to wild-type virus, but the C→S mutations were more severe. One explanation is that inserting a polar residue into the putative functional/catalytic site of E3 prevents proper protein association between E3 and its functional partner. However, inserting a more hydrophobic Ala, which in regard to charge is more similar to Cys, does not disrupt or interfere with this interaction as much.

Mutant E3 proteins that contained the PPCXPCC motif

TABLE 2. Infectivities of PPCXPCC motif mutants[a]

SINV	Mutation	Titer (PFU/ml)
Wild type	14 NVSFPCDR**P** **PTC**YTREPSRAL 34	8×10^9
PPCXPCC mutants		
SINV+PCV+C	14 NVSFPCDR**PPCVPCC**YTREPSRAL 37	1×10^{10}
SINV+C	14 NVSFPCDR**P** **PCC**YTREPSRAL 34	3×10^9
SINV+PCV	14 NVSFPCDR**PPCVPTC**YTREPSRAL 37	$<1 \times 10^1$
SINV+PCV revertant, SINV+PCV+P	14 NVSFPCDR**PPCVPPC**YTREPSRAL 37	3×10^8
T24P in WT SINV, SINV+P	14 NVSFPCDR**P** **PPC**YTREPSRAL 34	7×10^9

[a] BHK-21 cells were electroporated with equal amounts of in vitro-transcribed RNA. Virus was harvested at 24 h after electroporation, and titers were determined by plaque assay.

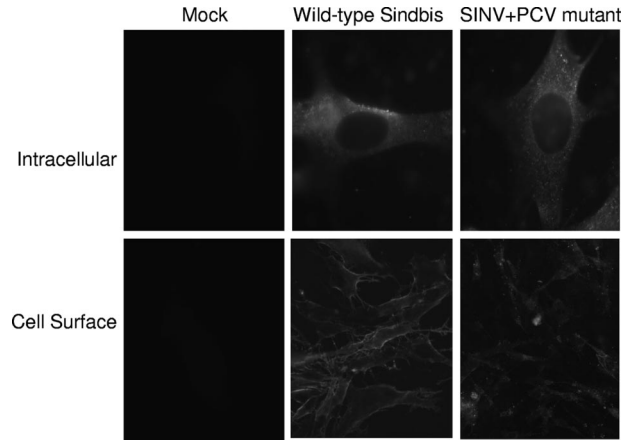

FIG. 5. Expression of pE2 and E2 protein in SINV+PCV. BHK-21 cells were transfected and after 8 h were fixed for intracellular staining (top) with 1.5% paraformaldehyde plus 0.01% Triton X-100 or for cell surface staining (bottom) with 1.5% paraformaldehyde. Cells were stained with an antibody recognizing E2. Cells intracellularly stained were imaged at a magnification of ×100 to show the internal staining pattern. Cells surface stained were imaged at a magnification of ×40 to show a larger distribution of cells.

found in some alphaviruses also had a mix of oxidized and reduced Cys residues. Furthermore, there was a correlation with the pattern of disulfide bonds and infectivity of the mutant virus. E3 proteins that contained single or sequential disulfide bonds (SINV, SINV+PCV+C, SINV+C, and SINV+PCV+P) produced infectious virus particles at wild-type titers. E3 proteins (SINV+PCV) that contained nested disulfide bonds did not produce infectious particles. Taken together, our results suggest that E3 has a functional role in virus assembly, because deletion, site-directed mutagenesis, and insertion of Cys residues into a specific region of E3 do not abolish virus assembly.

We hypothesize that the E3 protein is a viral protein disulfide isomerase that catalyzes the proper folding and disulfide bond formation in pE2/E2. E3 has labile disulfide bonds and is in close proximity to E2 throughout the assembly pathway. E2 contains 14 Cys residues in the ectodomain, most of which presumably form disulfide bonds. Assembly of spikes is a series of steps that occur in environments with different pHs. The reshuffling of disulfide bonds in pE2 (34), a possible result of the putative disulfide isomerase activity of E3, could be a key regulatory mechanism for spike formation. If E3 was functioning as a disulfide isomerase by forming intermolecular disulfide bonds with E2 during assembly, then the absence of one cysteine residue (Cys19 or Cys25) might not be as detrimental as the loss of both residues.

The rationale for a virus providing its own disulfide isomerase is to catalyze a reaction that occurs naturally, albeit more slowly, in the host. It has been shown that along with protein disulfide isomerase, calreticulin, calnexin, and ERp57 are all involved as chaperones in spike formation (33, 34, 36–38), suggesting that spike formation is a complex process which requires tremendous regulation during folding, heterodimerization, and assembly. By acting as a putative protein disulfide isomerase, E3 aids in folding the large quantity of E2 that is produced during a viral infection. It is known that if pE2 is not present in the ER, E1 will be degraded and will not be transported to the membrane. E3 ensures that pE2 is present so that the pE2-E1 heterodimerization can occur. E3 is cleaved in the trans-Golgi network only after heterodimerization of pE2 and E1, trimerization of the heterodimers, and spike assembly are completed. After this, E3 is dispensable.

Aside from other alphavirus E3 proteins, there are no known proteins that are similar to E3 based on amino acid sequence. Inspection of the E3 sequence reveals a Cys-X-X-Cys in the subset of alphaviruses that contain the PPCXPCC motif. This Cys-X-X-Cys sequence is shared by many redox proteins, including protein disulfide isomerase. Despite lacking any sequence similarity with one another, all of the Cys-X-X-Cys motif-containing proteins interact with cysteine-containing substrates (31, 51, 52). Further studies have shown that a Cys-Gly-Cys tripeptide is an efficient catalyst of disulfide isomerization despite not containing the Cys-X-X-Cys motif (50). Alphaviruses that do not contain the PPCXPCC motif do have a conserved Cys-X-X-Pro-Pro-X-Cys sequence, and putative protein disulfide isomerase activity may involve this sequence. Many nonviral proteins have Cys residues separated by 0 to 5 amino acids. These proteins include disulfide isomerases and redox-sensitive proteins (53). Like the unexpected Cys-Gly-Cys disulfide isomerase activity results, the putative disulfide isomerase activity of the Cys-X-X-Pro-Pro-X-Cys sequence will not be known until it is experimentally tested. These experiments are under way.

E3 is conserved in the alphavirus genome. If its sole purpose was to transport the E3-E2-6K-E1 polyprotein into the ER during folding, the signal sequence from E3 could have been integrated into E2 long ago. It is also clear that cleavage of E3 from E2 is required to form fusion-competent spikes. The hypothesis that E3 may function as a disulfide isomerase in the folding of E2 during assembly is consistent with the previous biochemical and genetic results as well as the data presented here.

ACKNOWLEDGMENTS

We thank Thomas Gallagher and Adam Zlotnick for helpful discussions and Christina Melki and Kaila Schollaert for technical assistance.

The National Center for Glycomics & Glycoproteomics is funded by NIH-NCRR grant 5P41RR018942 (to R.J.A.).

REFERENCES

1. **Andersson, H., B. U. Barth, M. Ekstrom, and H. Garoff.** 1997. Oligomerization-dependent folding of the membrane fusion protein of Semliki Forest virus. J. Virol. **71:**9654–9663.
2. **Barth, B. U., J. M. Wahlberg, and H. Garoff.** 1995. The oligomerization reaction of the Semliki Forest virus membrane protein subunits. J. Cell Biol. **128:**283–291.
3. **Bonatti, S., and G. Blobel.** 1979. Absence of a cleavable signal sequence in Sindbis virus glycoprotein PE2. J. Biol. Chem. **254:**12261–12264.
4. **Bonatti, S., G. Migliaccio, G. Blobel, and P. Walter.** 1984. Role of signal recognition particle in the membrane assembly of Sindbis viral glycoproteins. Eur. J. Biochem. **140:**499–502.
5. **Byrnes, A. P., and D. E. Griffin.** 1998. Binding of Sindbis virus to cell surface heparan sulfate. J. Virol. **72:**7349–7356.
6. **Carleton, M., and D. T. Brown.** 1996. Disulfide bridge-mediated folding of Sindbis virus glycoproteins. J. Virol. **70:**5541–5547.
7. **Carleton, M., H. Lee, M. Mulvey, and D. T. Brown.** 1997. Role of glycoprotein PE2 in formation and maturation of the Sindbis virus spike. J. Virol. **71:**1558–1566.
8. **Carugo, O., M. Cemazar, S. Zahariev, I. Hudaky, Z. Gaspari, A. Perczel, and S. Pongor.** 2003. Vicinal disulfide turns. Protein Eng. **16:**637–639.
9. **Cemazar, M., S. Zahariev, J. J. Lopez, O. Carugo, J. A. Jones, P. J. Hore, and S. Pongor.** 2003. Oxidative folding intermediates with nonnative disul-

fide bridges between adjacent cysteine residues. Proc. Natl. Acad. Sci. USA **100:**5754–5759.
10. **Cuff, J. A., M. E. Clamp, A. S. Siddiqui, M. Finlay, and G. J. Barton.** 1998. JPred: a consensus secondary structure prediction server. Bioinformatics **14:**892–893.
11. **de Curtis, I., and K. Simons.** 1988. Dissection of Semliki Forest virus glycoprotein delivery from the trans-Golgi network to the cell surface in permeabilized BHK cells. Proc. Natl. Acad. Sci. USA **85:**8052–8056.
12. **Gahmberg, C. G., G. Utermann, and K. Simons.** 1972. The membrane proteins of Semliki Forest virus have a hydrophobic part attached to the viral membrane. FEBS Lett. **28:**179–182.
13. **Garoff, H., A. M. Frischauf, K. Simons, H. Lehrach, and H. Delius.** 1980. Nucleotide sequence of cDNA coding for Semliki Forest virus membrane glycoproteins. Nature **288:**236–241.
14. **Garoff, H., D. Huylebroeck, A. Robinson, U. Tillman, and P. Liljestrom.** 1990. The signal sequence of the p62 protein of Semliki Forest virus is involved in initiation but not in completing chain translocation. J. Cell Biol. **111:**867–876.
15. **Garoff, H., K. Simons, and B. Dobberstein.** 1978. Assembly of the Semliki Forest virus membrane glycoproteins in the membrane of the endoplasmic reticulum in vitro. J. Mol. Biol. **124:**587–600.
16. **Garoff, H., K. Simons, and O. Renkonen.** 1974. Isolation and characterization of the membrane proteins of Semliki Forest virus. Virology **61:**493–504.
17. **Griffin, D. E.** 2001. Alphaviruses, p. 917–953. *In* D. M. Knipe and P. M. Howley (ed.), Fields virology. Lippincott Williams, Philadelphia, PA.
18. **Jain, S. K., S. DeCandido, and M. Kielian.** 1991. Processing of the p62 envelope precursor protein of Semliki Forest virus. J. Biol. Chem. **266:**5756–5761.
19. **Kalef, E., P. G. Walfish, and C. Gitler.** 1993. Arsenical-based affinity chromatography of vicinal dithiol-containing proteins: purification of L1210 leukemia cytoplasmic proteins and the recombinant rat c-erb A beta 1 T3 receptor. Anal. Biochem. **212:**325–334.
20. **Kao, P. N., and A. Karlin.** 1986. Acetylcholine receptor binding site contains a disulfide cross-link between adjacent half-cystinyl residues. J. Biol. Chem. **261:**8085–8088.
21. **Klimstra, W. B., K. D. Ryman, and R. E. Johnston.** 1998. Adaptation of Sindbis virus to BHK cells selects for use of heparan sulfate as an attachment receptor. J. Virol. **72:**7357–7366.
22. **Lescar, J., A. Roussel, M. W. Wien, J. Navaza, S. D. Fuller, G. Wengler, and F. A. Rey.** 2001. The fusion glycoprotein shell of Semliki Forest virus: an icosahedral assembly primed for fusogenic activation at endosomal pH. Cell **105:**137–148.
23. **Liljestrom, P., and H. Garoff.** 1991. Internally located cleavable signal sequences direct the formation of Semliki Forest virus membrane proteins from a polyprotein precursor. J. Virol. **65:**147–154.
24. **Lobigs, M., and H. Garoff.** 1990. Fusion function of the Semliki Forest virus spike is activated by proteolytic cleavage of the envelope glycoprotein precursor p62. J. Virol. **64:**1233–1240.
25. **Lobigs, M., J. M. Wahlberg, and H. Garoff.** 1990. Spike protein oligomerization control of Semliki Forest virus fusion. J. Virol. **64:**5214–5218.
26. **Lobigs, M., H. X. Zhao, and H. Garoff.** 1990. Function of Semliki Forest virus E3 peptide in virus assembly: replacement of E3 with an artificial signal peptide abolishes spike heterodimerization and surface expression of E1. J. Virol. **64:**4346–4355.
27. **Lopez, S., J. S. Yao, R. J. Kuhn, E. G. Strauss, and J. H. Strauss.** 1994. Nucleocapsid-glycoprotein interactions required for assembly of alphaviruses. J. Virol. **68:**1316–1323.
28. **Lustig, S., A. C. Jackson, C. S. Hahn, D. E. Griffin, E. G. Strauss, and J. H. Strauss.** 1988. Molecular basis of Sindbis virus neurovirulence in mice. J. Virol. **62:**2329–2336.
29. **Ma, L., C. T. Jones, T. D. Groesch, R. J. Kuhn, and C. B. Post.** 2004. Solution structure of dengue virus capsid protein reveals another fold. Proc. Natl. Acad. Sci. USA **101:**3414–3419.
30. **Mancini, E. J., M. Clarke, B. E. Gowen, T. Rutten, and S. D. Fuller.** 2000. Cryo-electron microscopy reveals the functional organization of an enveloped virus, Semliki Forest virus. Mol. Cell **5:**255–266.
31. **Martin, J. L.** 1995. Thioredoxin—a fold for all reasons. Structure **3:**245–250.
32. **Mayne, J. T., C. M. Rice, E. G. Strauss, M. W. Hunkapiller, and J. H. Strauss.** 1984. Biochemical studies of the maturation of the small Sindbis virus glycoprotein E3. Virology **134:**338–357.
33. **Molinari, M., and A. Helenius.** 2000. Chaperone selection during glycoprotein translocation into the endoplasmic reticulum. Science **288:**331–333.
34. **Molinari, M., and A. Helenius.** 1999. Glycoproteins form mixed disulphides with oxidoreductases during folding in living cells. Nature **402:**90–93.
35. **Mukhopadhyay, S., W. Zhang, S. Gabler, P. R. Chipman, E. Lenches, J. H. Strauss, T. S. Baker, R. J. Kuhn, and M. G. Rossmann.** 2006. Mapping the structure and function of the E1 and E2 glycoproteins in alphaviruses. Structure **14:**63–73.
36. **Mulvey, M., and D. T. Brown.** 1996. Assembly of the Sindbis virus spike protein complex. Virology **219:**125–132.
37. **Mulvey, M., and D. T. Brown.** 1994. Formation and rearrangement of disulfide bonds during maturation of the Sindbis virus E1 glycoprotein. J. Virol. **68:**805–812.
38. **Mulvey, M., and D. T. Brown.** 1995. Involvement of the molecular chaperone BiP in maturation of Sindbis virus envelope glycoproteins. J. Virol. **69:**1621–1627.
39. **Omar, A., and H. Koblet.** 1988. Semliki Forest virus particles containing only the E1 envelope glycoprotein are infectious and can induce cell-cell fusion. Virology **166:**17–23.
40. **Owen, K. E., and R. J. Kuhn.** 1996. Identification of a region in the Sindbis virus nucleocapsid protein that is involved in specificity of RNA encapsidation. J. Virol. **70:**2757–2763.
41. **Piotto, M., V. Saudek, and V. Sklenar.** 1992. Gradient-tailored excitation for single-quantum NMR spectroscopy of aqueous solutions. J. Biomol. NMR **2:**661–665.
42. **Pletnev, S. V., W. Zhang, S. Mukhopadhyay, B. R. Fisher, R. Hernandez, D. T. Brown, T. S. Baker, M. G. Rossmann, and R. J. Kuhn.** 2001. Locations of carbohydrate sites on alphavirus glycoproteins show that E1 forms an icosahedral scaffold. Cell **105:**127–136.
43. **Rice, C. M., J. R. Bell, M. W. Hunkapiller, E. G. Strauss, and J. H. Strauss.** 1982. Isolation and characterization of the hydrophobic COOH-terminal domains of the Sindbis virion glycoproteins. J. Mol. Biol. **154:**355–378.
44. **Salminen, A., J. M. Wahlberg, M. Lobigs, P. Liljestrom, and H. Garoff.** 1992. Membrane fusion process of Semliki Forest virus. II. Cleavage-dependent reorganization of the spike protein complex controls virus entry. J. Cell Biol. **116:**349–357.
45. **Smith, T. J., R. H. Cheng, N. H. Olson, P. Peterson, E. Chase, R. J. Kuhn, and T. S. Baker.** 1995. Putative receptor binding sites on alphaviruses as visualized by cryoelectron microscopy. Proc. Natl. Acad. Sci. USA **92:**10648–10652.
46. **Wahlberg, J. M., W. A. Boere, and H. Garoff.** 1989. The heterodimeric association between the membrane proteins of Semliki Forest virus changes its sensitivity to low pH during virus maturation. J. Virol. **63:**4991–4997.
47. **Wahlberg, J. M., and H. Garoff.** 1992. Membrane fusion process of Semliki Forest virus. I. Low pH-induced rearrangement in spike protein quaternary structure precedes virus penetration into cells. tJ. Cell Biol. **116:**339–348.
48. **Wang, X., M. Connor, R. Smith, M. W. Maciejewski, M. E. Howden, G. M. Nicholson, M. J. Christie, and G. F. King.** 2000. Discovery and characterization of a family of insecticidal neurotoxins with a rare vicinal disulfide bridge. Nat. Struct. Biol. **7:**505–513.
49. **Welch, W. J., and B. M. Sefton.** 1979. Two small virus-specific polypeptides are produced during infection with Sindbis virus. J. Virol. **29:**1186–1195.
50. **Woycechowsky, K. J., and R. T. Raines.** 2003. The CXC motif: a functional mimic of protein disulfide isomerase. Biochemistry **42:**5387–5394.
51. **Woycechowsky, K. J., and R. T. Raines.** 2000. Native disulfide bond formation in proteins. Curr. Opin. Chem. Biol. **4:**533–539.
52. **Woycechowsky, K. J., K. D. Wittrup, and R. T. Raines.** 1999. A small-molecule catalyst of protein folding in vitro and in vivo. Chem. Biol. **6:**871–879.
53. **Zhang, R. M., and G. H. Snyder.** 1989. Dependence of formation of small disulfide loops in two-cysteine peptides on the number and types of intervening amino acids. J. Biol. Chem. **264:**18472–18479.
54. **Zhang, W., S. Mukhopadhyay, S. V. Pletnev, T. S. Baker, R. J. Kuhn, and M. G. Rossmann.** 2002. Placement of the structural proteins in Sindbis virus. J. Virol. **76:**11645–11658.
55. **Zhang, X., M. Fugere, R. Day, and M. Kielian.** 2003. Furin processing and proteolytic activation of Semliki Forest virus. J. Virol. **77:**2981–2989.